Published February 15, 2013

Special Section: Frozen Soils

Yuki Kojima*
Joshua L. Heitman
Gerald N. Flerchinger
Robert Horton

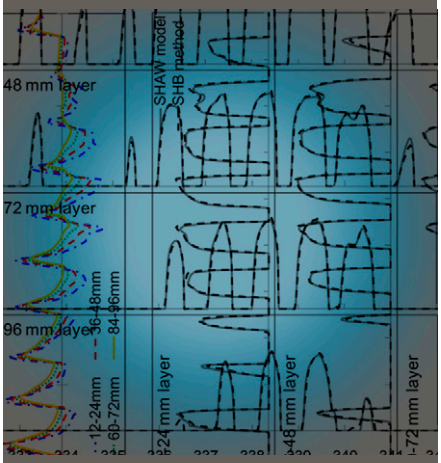

The applicability of the sensible heat balance (SHB) concept for estimating soil freezing and thawing rates was tested in a numerical modeling study. Results indicated that the SHB method was suitable for estimating soil freezing and thawing rates at depths below 24 mm. Application of the method requires accurate estimates of soil thermal properties.

Y. Kojima and R. Horton, Agronomy Dep., Iowa State Univ., Ames, IA 50011; J.L. Heitman, Soil Science Dep., North Carolina State Univ., Raleigh, NC 27695; and G.N. Flerchinger, USDA-ARS, Northwest Watershed Research center, Boise, ID 83712. *Corresponding author (ykojima@iastate.edu).

Vadose Zone J.
doi:10.2136/vzj2012.0053
Received 27 Apr. 2012.

Numerical Evaluation of a Sensible Heat Balance Method to Determine Rates of Soil Freezing and Thawing

In situ determination of soil freezing and thawing is difficult despite its importance for many environmental processes. A sensible heat balance (SHB) method using a sequence of heat pulse probes has been shown to accurately measure water evaporation in subsurface soil, and it has the potential to measure soil freezing and thawing. Determination of soil freezing and thawing may be more challenging than evaporation, however, because the latent heat of fusion is smaller than the latent heat of vaporization. Furthermore, convective heat flow associated with liquid water flow and occurrence of evaporation or condensation during freezing and thawing may cause inaccurate estimation of freezing and thawing with the SHB method. The objective of this study was to examine the applicability of the SHB concept to soil freezing and thawing. Soil freezing and thawing events were simulated with the simultaneous heat and water (SHAW) model. Ice contents were estimated by applying the SHB concept to numerical data produced by the SHAW model. Close agreement between the SHB-estimated and the SHAW-simulated ice contents were observed at depths below 24 mm. The main cause of inaccuracies with the SHB method was poor estimation of heat conduction at the 12-mm depth, possibly due to simplifications of temporal or vertical distributions of temperature and thermal conductivity. The effects of convective heat flow and concurrent evaporation or condensation and freezing or thawing on the SHB method were small. The results indicate that the SHB method is conceptually suitable for estimating soil freezing and thawing. Independent, accurate estimates of thermal properties must be available to effectively use the SHB method to determine in situ soil freezing and thawing.

Abbreviations: DOY, day of the year; SHAW, simultaneous heat and water; SHB, sensible heat balance.

Soil freezing and thawing have critical effects on water and chemical movement in the soil during winter and spring. Ice in partially frozen soil can interrupt the infiltration of rainfall or snowmelt, leading to surface runoff and erosion (Kane and Stein, 1983; Cruse et al., 2001). Furthermore, frozen soils have a low matric potential similar to dry soils (Williams, 1964; Koopmans and Miller, 1966), so that liquid water flow from warm layers into cold layers, generally upward in direction, is induced (Dirksen and Miller, 1966; Kung and Steenhuis, 1986). Simultaneously, liquid water flow causes advective movement of dissolved chemicals (Cary and Mayland, 1972; Cary et al., 1979; Galinato, 1987). Liquid water moving upward into colder layers causes increasing ice content in the freezing zone. Moreover, the formation of ice lenses by freezing results in soil structural changes (Penner, 1967; Miller, 1972; Gieselman et al., 2008). Hence, determining water contents, water flow rates, and water-to-ice phase changes in partially frozen soils is important.

Continuous in situ measurement of unfrozen water content has been successful using dielectric permittivity measurements such as time-domain reflectometry (TDR) (Stein and Kane, 1983; Hayhoe et al., 1983; Spaans and Baker, 1995). It has been reported that the relationship between dielectric permittivity of partially frozen soils and liquid water content is dependent on the total water content so that calibrations taking into account ice permittivity are required for accurate measurements (Spaans and Baker, 1995; Seyfried and Murdock, 1996; Watanabe and Wake, 2009). Temporal in situ measurements of ice formation and thawing in soil have been difficult to obtain in spite of their importance. Few studies on estimating the soil volumetric ice content have been reported. Kelleners and Norton (2012) estimated the volumetric ice content with a dielectric permittivity sensor and a dielectric mixing model (Bittelli et al., 2003). They assumed that the total water content did not change during soil freezing. That assumption ignores liquid water supplied from snow cover or by liquid water flow in partially frozen soil. Bittelli et al. (2004) examined a mixing model used in conjunction with dielectric permittivities measured at two different frequencies. The method was

successful for low clay content soils only. The total water content in partially frozen soil can be measured with a γ radiation attenuation method (Loch and Kay, 1978; Fukuda, 1983) or a neutron probe method (Sartz, 1969; Fukuda and Kinosita, 1985). Thus, ice and water contents may be determined simultaneously by combining γ radiation attenuation or neutron probe measurements with dielectric permittivity measurements (Hayhoe and Bailey, 1985; Kahimba and Sri Ranjan, 2007). There are difficulties in using γ radiation under field conditions, however, and neutron probe measurements are for relatively large volumes of soil that do not match in scale with the TDR measurements. Watanabe et al. (2010), Liu and Si (2011), and Zhang et al. (2011) examined the estimation of ice content from volumetric heat capacity measured with a heat pulse probe but encountered problems with estimations near 0°C. Clearly, there is a need for improved field measurement techniques for estimating water and ice contents.

A SHB method using a sequence of heat pulse probes positioned with depth has been shown to accurately measure water evaporation and condensation at shallow soil depths (Heitman et al., 2008a, 2008c; Xiao et al., 2011), and the applicability of the SHB has been confirmed by a numerical study (Sakai et al., 2011). It is possible to apply the SHB method to soil freezing and thawing to determine ice content changes when the latent heat of fusion is the main source of latent heat in the soil. A potential advantage of the SHB method is that it provides both water transfer and heat transfer information with relatively simple measurements, e.g., ambient temperature changes and local temperature changes in response to heater inputs. The SHB method can potentially measure freezing at a millimeter to centimeter depth scale. The measurement of soil freezing and thawing may be more challenging, however, than measuring evaporation and condensation because (i) the latent heat of fusion (334,000 J kg^{-1} at 0°C) is much smaller than the latent heat of vaporization (2,442,000 J kg^{-1} at 25°C), (ii) soil freezing and thawing generates liquid water flow, which contributes to heat transfer that has not been explicitly accounted for in previous applications of the SHB method for evaporation and condensation, and (iii) concurrence of evaporation–condensation and freezing–thawing may cause inaccurate estimation of the ice content with the SHB method because it cannot distinguish the latent heat of vaporization and the latent heat of fusion.

Because of the potential benefits of estimating changing ice contents with depth and time, it is important to evaluate the possibility of using a SHB method to determine the rates of soil freezing and thawing. Therefore, the objective of this study was to examine the conceptual applicability and potential limitations of the SHB method to determine soil freezing and thawing by numerical analysis. The numerical study consisted of two steps. In Step 1, soil freezing and thawing events were simulated with the SHAW model. In Step 2, the SHB method was used to analyze the data numerically generated with the SHAW model. The applicability and potential limitations of the SHB method were investigated by comparing the SHB method estimations of ice contents with ice contents calculated by the SHAW model. The SHB calculations assume that heat pulse probes can accurately measure the thermal properties of partially frozen soils and that heat pulse inputs by heat pulse probes are a negligible source of heat in the heat balance.

Theory

Sensible Heat Balance Method

Heat pulse probes are widely used to determine soil thermal properties (volumetric heat capacity, thermal diffusivity, and thermal conductivity) (Campbell et al., 1991; Kluitenberg et al., 1995; Ochsner et al., 2001). Sensible heat balance terms for soil layers (Heitman et al., 2008a, 2008c), i.e., sensible heat inflow, sensible heat outflow, and the change in sensible heat storage, can be determined with a heat pulse probe (Fig. 1). Conductive heat fluxes at the upper and lower boundaries of a specified soil layer, H_u and H_l (W m^{-2}), are described as

$$H_u = -\lambda_u \frac{T_i - T_{i-1}}{\Delta z}, \quad H_l = -\lambda_l \frac{T_{i+1} - T_i}{\Delta z} \qquad [1]$$

where λ_u and λ_l are thermal conductivities (W m^{-1} °C^{-1}) at the upper and lower boundaries, respectively, T_i is temperature at the depth i of each temperature sensor (°C), and Δz is the difference in depth of the temperature sensors (m). The change in sensible heat storage of the layer, ΔS (W m^{-2}), is written as

$$\Delta S = \left(\frac{C_u + C_l}{2}\right)\frac{\Delta T_i}{\Delta t}\Delta z \qquad [2]$$

where C_u and C_l are volumetric heat capacities (J m^{-3} °C^{-1}) in the soil above and below the heating needle, ΔT_i is the temperature change of the ith soil layer with time (°C), and Δt is the time step interval (s). The values of C_u and C_l are averaged to estimate the

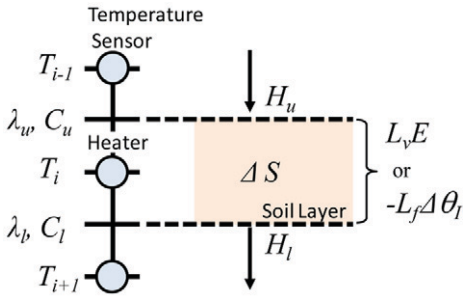

Fig. 1. Diagram of the sensible heat balance method with heat pulse probe measurements to determine the latent heat of vaporization or fusion of a specific soil layer i. Symbols denote temperature (T), thermal conductivity (λ), heat capacity (C), sensible heat flux (H), change in heat storage (ΔS), latent heat of vaporization (L_v), latent heat of fusion (L_f), evaporation rate (E), and change in ice content ($\Delta\theta_l$). The subscripts u and l represent upper and lower boundaries, respectively.

volumetric heat capacity at the center of the layer. The thermal conductivity λ and the volumetric heat capacity C are determined from temperature transitions at the adjacent sensing needles above and below the heating needle corresponding to the heat input at the center needle (Bristow et al., 1994). Heat pulse probes used in previous research for the SHB method (Heitman et al., 2008a, 2008c) were designed with 6-mm needle intervals. Therefore, the soil layer thickness can be 6 mm or multiples of 6 mm. Measuring thermal properties accurately in partially frozen soils is challenging because ice melts when heat is applied (Putkonen, 2003; Overduin et al., 2006; Ochsner and Baker, 2008; Watanabe et al., 2010; Tokumoto et al., 2010; Wagner-Riddle et al., 2010). Further investigation and improvement in measuring the thermal properties of partially frozen soils is warranted.

Because water evaporation and condensation or water freezing and thawing involve large amounts of latent heat, the residual or hidden heat associated with water phase changes must be included in a sensible heat balance calculation for a specific soil layer. Evaporation and condensation rates of water can be determined by dividing the missing or excess heat by the latent heat of vaporization when the soil temperature is >0°C, and the missing or excess heat can be considered as the latent heat produced or consumed by soil freezing or thawing when the soil temperature is <0°C:

$$\begin{aligned} (H_u - H_l) - \Delta S &= L_v E_i \qquad T > 0^\circ\mathrm{C} \\ (H_u - H_l) - \Delta S &= -L_f \Delta\theta_I \qquad T < 0^\circ\mathrm{C} \end{aligned} \qquad [3]$$

where L_v is the latent heat of vaporization (J m^{-3}), E_i is the evaporation rate from the specific layer i (m s^{-1}), L_f is the latent heat of fusion (J m^{-3}), and $\Delta\theta_I$ is the change in ice content in the layer (m s^{-1}). Although the excess heat or missing heat term also includes convective heat associated with liquid water and vapor flows, the SHB method assumes that convective heat transfer is negligible. Sakai et al. (2011) reported that this assumption is acceptable when the SHB method is used for evaporation and condensation. When the soil temperature is <0°C, not only do freezing and thawing occur, but it is possible for evaporation or sublimation and condensation to also occur. Thus, Eq. [3] for freezing and thawing may not be effective for determining ice content changes when soil water evaporation or sublimation rates are significant during freezing and thawing.

Numerical Simulation

Soil freezing and thawing events were simulated numerically with the SHAW model. The SHAW model is a one-dimensional finite-difference model that simulates coupled heat, water, and solute transfer in atmosphere–plant–snow–residue–soil systems (Flerchinger and Saxton, 1989a) and has been widely applied to in situ soil freezing and thawing events (Flerchinger and Saxton, 1989b; Nassar et al., 2000; Flerchinger et al., 2006). In this study, the surface was fixed as a bare soil surface, i.e., only soil and atmosphere were included in the system. Additionally, the model, usually used with 1-h time steps, was modified to operate and output results at 1-min time steps. A one-dimensional water balance equation including liquid water flow and vapor flow in the soil is expressed by the SHAW model as (Flerchinger and Saxton, 1989a)

$$\frac{\partial\theta_L}{\partial t} + \frac{\rho_I}{\rho_L}\frac{\partial\theta_I}{\partial t} = \frac{\partial}{\partial z}\left[K\left(\frac{\partial\psi}{\partial z} + 1\right)\right] + \frac{1}{\rho_L}\frac{\partial q_v}{\partial z} \qquad [4]$$

where t is time (s), θ are volume water contents (m^3 m^{-3}), ρ are densities (kg m^{-3}), z is depth (m), K is hydraulic conductivity (m s^{-1}), ψ is the soil water matric potential (m H_2O), q is water flux (m s^{-1}), and the subscripts L, I, and v designate liquid water, ice, and water vapor, respectively. The relationship between matric potential ψ and volumetric liquid water content θ_L is expressed as (Campbell, 1974)

$$\psi = \psi_e\left(\frac{\theta_L}{\theta_s}\right)^{-b} \qquad [5]$$

where θ_s is saturated soil water content (m^3 m^{-3}) and ψ_e and b are air entry potential (m H_2O) and a pore size distribution index, respectively, which are obtained by curve fitting Eq. [5] to experimental observations. Determination of the soil hydraulic conductivity K as a function of matric potential or water content uses the parameters defined in Eq. [5] (Campbell, 1974),

$$K = K_s\left(\frac{\psi_e}{\psi}\right)^{2+(3/b)} = K_s\left(\frac{\theta_L}{\theta_s}\right)^{2b+3} \qquad [6]$$

where K_s is the saturated hydraulic conductivity (m s^{-1}). When ice is present in the soil, the matric potential ψ is expressed as a function of temperature (Fuchs et al., 1978):

$$\psi = \frac{L_f}{g}\left(\frac{T}{T + 273.16}\right) \qquad [7]$$

where g is gravitational acceleration (9.81 m s^{-2}) and T is the temperature (°C). By combining Eq. [5] and [7], the maximum liquid water content can be defined, and the ice content is the difference between the total water content and the maximum liquid water content. When the total water content θ_T is smaller than the maximum liquid water content, the liquid water content is equal to θ_T and the ice content is considered to be zero.

The governing one-dimensional energy conservation equation including soil freezing and thawing, heat conduction, and convective heat transfer with both liquid water and vapor is (Flerchinger and Saxton, 1989a)

$$C_s\frac{\partial T}{\partial t}-\rho_I L_f\frac{\partial \theta_I}{\partial t}= \frac{\partial}{\partial z}\left(\lambda_s\frac{\partial T}{\partial z}\right)-\rho_L c_L\frac{\partial (q_L T)}{\partial z}-L_v\left(\frac{\partial q_v}{\partial z}+\frac{\partial \rho_v}{\partial t}\right) \quad [8]$$

where C_s is the soil volumetric heat capacity (J m^{-3} °C^{-1}), λ_s is the soil thermal conductivity (W m^{-1} °C^{-1}), and c_L is the specific heat of liquid water (J kg^{-1} °C^{-1}). The thermal conductivity λ_s and volumetric heat capacity C_s of soils are calculated as functions of the soil particle size distribution, organic matter content, bulk density, soil liquid water content, and ice content using the theory initially developed by de Vries (1963) and modified for partially frozen soil by Penner (1970):

$$\lambda_s=\frac{\sum m_j\lambda_j\theta_j}{\sum m_j\theta_j} \quad [9]$$

$$C_s=\sum\rho_j c_j\theta_j \quad [10]$$

where m is weighting factor, λ is the thermal conductivity (W m^{-1} °C^{-1}), ρ is density (kg m^{-3}), c is the specific heat (J kg^{-1} °C^{-1}), and θ is the volume fraction (m^3 m^{-3}) of each soil constituent j (minerals, organic matter, water, ice, and air). The surface boundary condition of the system is determined by the surface energy balance equation:

$$R_n=H_{sf}+L_vE_{sf}+G \quad [11]$$

where R_n is net radiation (W m^{-2}), H_{sf} is the sensible heat flux at the surface (W m^{-2}), E_{sf} is the evaporation rate at the surface (m s^{-1}), and G is the ground heat flux (W m^{-2}). The values of R_n, H_{sf}, and E_{sf} are determined from weather and surface conditions; R_n is defined as (Campbell and Norman, 1998)

$$R_n=(1-\alpha)R_s+\sigma\varepsilon_s\left(\varepsilon_a T_a^4-T_{sf}^4\right) \quad [12]$$

where α is the surface albedo, R_s is solar radiation (W m^{-2}), σ is the Stefan–Boltzmann constant (5.67 × 10^{-8} W m^{-2} K^{-4}), ε_s is emissivity of the surface, ε_a is the atmospheric emissivity, T_{sf} is the surface temperature (°C), and T_a is the air temperature (°C). The values of H_{sf} and E_{sf} are determined by (Campbell and Norman, 1998)

$$H_{sf}=\rho_a c_a\frac{T_{sf}-T_a}{r_H} \quad [13]$$

$$E_{sf}=\frac{\rho_{vs}-\rho_{va}}{r_v} \quad [14]$$

where ρ_a and c_a are the density (kg m^{-3}) and specific heat (J kg^{-1} °C^{-1}) of air, r_H is resistance to surface heat transfer (s m^{-1}), ρ_{vs} and ρ_{va} are the vapor densities of the surface and atmosphere (kg m^{-3}), respectively, and r_v is resistance to vapor transfer (s m^{-1}), which is taken to be equal to r_H. The vapor density of the surface and atmosphere are determined by multiplying the relative humidity and saturated vapor density at the appropriate temperatures. The value of r_H is calculated as a function of wind speed u (m s^{-1}) (Campbell and Norman, 1998):

$$r_H=\frac{1}{uk^2}\left[\ln\left(\frac{z_{ref}-d+z_H}{z_H}\right)+\Psi_H\right]\times\left[\ln\left(\frac{z_{ref}-d+z_m}{z_m}\right)+\Psi_m\right] \quad [15]$$

where k is von Karman's constant, z_{ref} is the measurement height (m), d is the zero plane displacement (m), z_H and z_m are the surface roughness parameter for the temperature and momentum profile (m), respectively, and Ψ_H and Ψ_m are the profile diabatic correction factors for heat and momentum, which are a function of atmospheric stability. The value of G is determined as a residual that satisfies the energy balance equation, Eq. [11]; G and E_{sf} are used at each time step in the SHAW model as the upper boundary conditions of total heat flux and total water flux, respectively.

Materials and Methods

Calculations for a Step Change in Air Temperature Conditions

Soil freezing and thawing events for two soils, Hanlon sand and Ida silt loam, were simulated for a step change in air temperature conditions. Each soil's texture, bulk density, organic matter content, and parameters for thermal properties and hydraulic properties are shown in Table 1. The air relative humidity RH_a is set at 50%, and the air temperature T_a is maintained at −5°C for a 96 h simulation period, and re-set to 5°C after the first 96 h until the soil ice content becomes zero:

$$T_{a(t)}=\begin{cases}-5°C & t<96\text{ h}\\ 5°C & t\geq 96\text{ h}\end{cases} \quad [16]$$

The other weather conditions, solar radiation R_s, wind speed u (m s^{-1}), and precipitation rate P (mm h^{-1}) are set at zero during the simulation. The lower boundary condition is defined by maintaining the initial soil temperature and volumetric water content constant throughout the simulation period. The initial soil temperature $T_{(z,0)}$ was 5°C, and initial soil volumetric water contents $\theta_{L(z,0)}$ were chosen as 0.05 m^3 m^{-3} or 0.10 m^3 m^{-3} for Hanlon sand and 0.20 m^3 m^{-3} or 0.30 m^3 m^{-3} for Ida silt loam:

$$T_{(z,0)}=5°C$$
$$\theta_{L(z,0)}=\begin{cases}0.05\text{ or }0.10\text{ m}^3\text{m}^{-3} & (\text{sand})\\ 0.20\text{ or }0.30\text{ m}^3\text{m}^{-3} & (\text{silt loam})\end{cases} \quad [17]$$

Table 1. Particle size distribution, organic matter content, bulk density, and soil hydraulic parameters used in the simultaneous heat and water (SHAW) model calculations. The sand and silt loam data were taken from Heitman et al. (2008b), and the loamy sand data were taken from Flerchinger et al. (2006).

Soil	Textural fractions			Organic matter	Bulk density	Hydraulic parameters†			
	Sand	Silt	Clay			ψ_e	b	θ_s	K_s
	kg kg^{-1}				kg m^{-3}	m		m^3 m^{-3}	m s^{-1}
Sand	0.917	0.072	0.011	0.006	1600	0.03	3.38	0.396	9.8×10^{-6}
Silt loam	0.022	0.729	0.249	0.044	1200	0.13	6.53	0.547	3.8×10^{-6}
Loamy sand	0.896	0.080	0.024	0.005	1624	0.13	3.16	0.390	3.4×10^{-5}

† ψ_e, air-entry potential; b, pore size distribution index; θ_s, saturated water content; K_s, saturated hydraulic conductivity.

The $\theta_{L\,(z,0)}$, 0.10 m^3 m^{-3} for Hanlon sand and 0.30 m^3 m^{-3} for Ida silt loam, are approximate water content at field capacity ($\psi \approx -3.40$ m H_2O). The $\theta_{L\,(z,0)}$, 0.05 m^3 m^{-3} for Hanlon sand and 0.20 m^3 m^{-3} for Ida silt loam, were chosen to represent drier than field capacity conditions. The simulated soil profile covered the depth increment 0 to1 m. Node spacing was 0.006 m in the 0-0.18 m soil layer, and node spacing gradually increased in deeper soil to a distance of 0.1 m for the deepest nodes ending at 1 m. Soil temperature T, total water content θ_T, ice content θ_I, thermal conductivity λ_s, and volumetric heat capacity C_s values for each simulated minute are provided by the SHAW model. T is given as a result of numerically solving Eq. [8]. θ_T, and θ_I, are determined by the numerical solution of Eq. [4] combined with Eq. [5], [6], and [7]. λ_s and C_s are computed with Eq. [9] and [10], respectively.

Calculation with Transient Atmospheric Conditions

A simulation under transient atmospheric conditions was performed to further examine the applicability of the sensible heat balance method for estimating soil freezing and thawing in response to environment changes. Hourly weather data for the Orchard site (43°19′ N, 115°59′ W), described in detail by Flerchinger and Hardegree (2004) and Flerchinger et al. (2006), were used for this study. The weather data consisted of T_a, RH_a, u, R_s, and P. Tindahay loamy sand was the main soil at the site (Table 1). This study focused on soil freezing and thawing between day of the year, DOY, 332 (28 Nov.) and DOY 342 (8 Dec.), 1997. The actual simulation started with data from DOY 309 (5 Nov.), 1997, to establish realistic distributions of temperature and water content for the study period. The same node spacings and soil depths as used with the step change in air conditions simulations were used for these transient condition simulations. The initial condition was established by linearly interpolating soil temperatures measured at depths of 0.01, 0.02, 0.05, 0.10, 0.20, 0.30, 0.50 and 1.00 m, and linearly interpolating soil water contents measured at depths of 0.02, 0.05, 0.10, 0.20, 0.30, 0.50 and 1.00 m on DOY 309, 1997. The lower boundary condition was maintained constant for temperature and soil water content, 13.4°C and 0.081 m^3 m^{-3}, respectively.

Application of the Sensible Heat Balance Method

The numerically produced data from the SHAW model, e.g., soil temperature T, thermal conductivity λ_s, and volumetric heat capacity C_s, for each 15 min simulated time were used for SHB method applications (Eq. [3]) to calculate temporal changes in ice contents θ_I. Each 12 mm subsurface soil layer from 12 mm to 168 mm depth was evaluated (12–24, 24–36, 36–48, 48–60, 60–72, 72–84, 84–96, 96–108, 108–120, 120–132, 132–144, 144–156, 156–168 mm). Since soil freezing penetrates much deeper than soil subsurface evaporation, a 12 mm soil layer thickness was chosen. The 12 mm soil layer thickness is representative of the spacing of a 3 needle heat pulse probes. Thus, 12-mm soil layer thickness is a convenient thickness with practical application. As the uppermost depth increment, the 0–12 mm soil layer was not included in the analysis because heat pulse probes cannot measure the surface thermal gradient as a finite difference across the soil surface, i.e., needles can't be placed above and below the soil surface to determine a gradient (Fig. 1; Heitman et al., 2008a). Thus, the method is only potentially applicable to estimate latent heat in the subsurface.

Results and Discussion

Sensible Heat Balance for a Step Change in Air Temperature Condition

The ice content time series calculated with the SHB method for each soil layer were compared with the ice content time series calculated with the SHAW model at the center node of each soil layer (18, 30, 42, 54, 66, 78, 90, 102, 114, 126, 138, 150, and 162 mm). Results for the 12- to 24-, 36- to 48-, 60- to 72-, and 84- to 96-mm soil layers are presented with soil temperatures at the center node of each soil layer calculated with the SHAW model in Fig. 2 and 3 for sand and silt loam, respectively. Ice contents in both sand and silt loam increased as the soil temperature decreased and became stable after the initial rapid increase. In Fig. 2 and 3, the maximum values are shown in proportion to the initial water contents $\theta_{L(z,0)}$. Maximum absolute differences between the ice content simulated with the SHAW model and the ice content calculated with the SHB method during the freezing and thawing event for the 12- to 24-, 36- to 48-, 60- to 72-, and 84- to 96-mm soil layers,

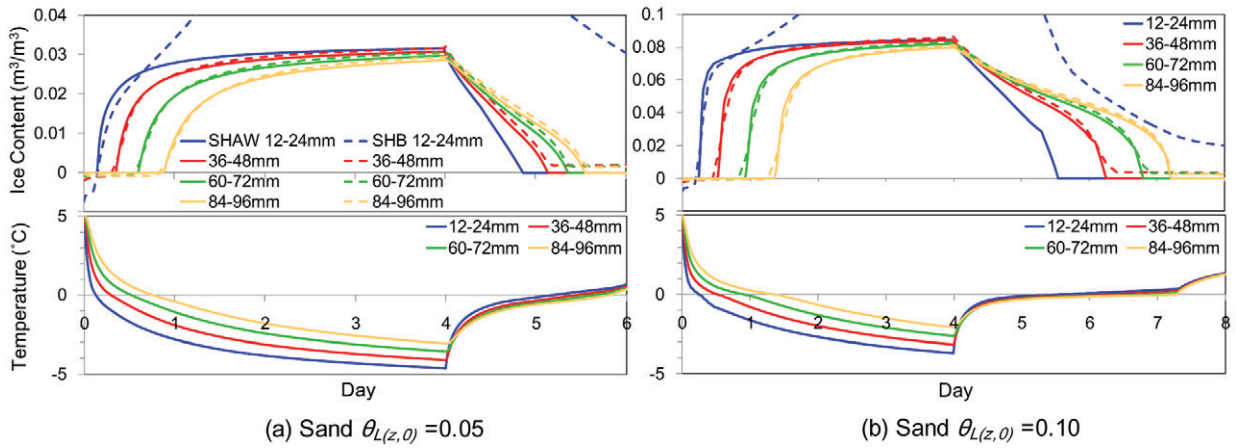

Fig. 2. Volumetric ice contents simulated with the simultaneous heat and water (SHAW) model (solid lines) and calculated with the sensible heat balance (SHB) method (dashed lines) for a step change in air temperature conditions (upper), and temperature simulated with the SHAW model (lower) for sand with an initial water content [$\theta_{L(z,0)}$] of (a) 0.05 m^3 m^{-3} and (b) 0.10 m^3 m^{-3} for the 12- to 24-, 36- to 48-, 60- to 72-, and 84- to96-mm soil layers.

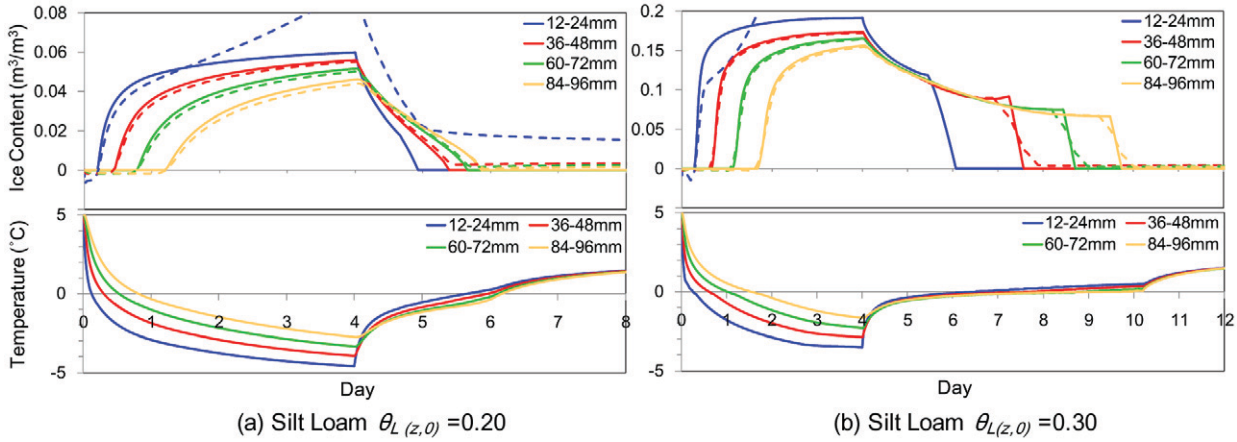

Fig. 3. Volumetric ice contents simulated with the simultaneous heat and water (SHAW) model (solid lines) and calculated with the sensible heat balance (SHB) method (dashed lines) for a step change in air temperature conditions (upper) and temperature simulated with the SHAW model (lower) for silt loam with an initial water content [$\theta_{L(z,0)}$] of (a) 0.20 m^3 m^{-3} and (b) 0.30 m^3 m^{-3} for the 12- to 24-, 36- to 48-, 60- to 72-, and 84- to96-mm soil layers.

respectively, were 0.154, 0.003, 0.003, and 0.002 m^3 m^{-3} for the sand with $\theta_{L(z,0)}$ = 0.05 m^3 m^{-3}; 0.127, 0.012, 0.011, and 0.010 m^3 m^{-3} for the sand with $\theta_{L(z,0)}$ = 0.10 m^3 m^{-3}; 0.035, 0.004, 0.003, and 0.003 m^3 m^{-3} for the silt loam with $\theta_{L(z,0)}$ = 0.20 m^3 m^{-3}; and 0.444, 0.026, 0.020, and 0.018 m^3 m^{-3} for the silt loam with $\theta_{L(z,0)}$ = 0.30 m^3 m^{-3}. The absolute differences are quite small except for the shallowest soil layer (12–24 mm). The ice contents of the 12- to 24-mm layer estimated with the SHB method for the sand with $\theta_{L(z,0)}$ = 0.05 and 0.10 m^3 m^{-3} and the silt loam with $\theta_{L(z,0)}$ = 0.20 and 0.30 m^3 m^{-3} had maximum values of 0.122, 0.211, 0.094, and 0.635 m^3 m^{-3}, respectively. The deeper the soil layer, the smaller the maximum absolute difference. Moreover, larger maximum absolute differences are shown for larger initial soil water contents.

The differences between the SHB method and the SHAW calculations may have been caused by (i) the SHB method not accounting for convective heat flow associated with liquid and vapor water transfer, (ii) simultaneous evaporation–condensation and freezing–thawing, and (iii) calculation errors of sensible heat flux H and sensible heat storage ΔS.

Although the ice content transitions for the 12- to 24-mm soil layer were not accurately described by the SHB method, the SHAW model ice content determination and SHB method ice content were consistent in depth and time for the soil layers deeper than 24 mm. The absolute differences for the soil layers deeper than 24 mm are quite small, being at most 0.003, 0.012, 0.004, and 0.026 m^3 m^{-3} for the sand with $\theta_{L(z,0)}$ = 0.05 and 0.10 m^3 m^{-3} and the silt loam with $\theta_{L(z,0)}$ = 0.20 and 0.30 m^3 m^{-3}, respectively. The

slightly larger errors for the silt loam with $\theta_{L(z,0)} = 0.30$ m^3 m^{-3} are due to differences in the timing and rate of soil thawing (Days 7–10) in Fig. 3b. The magnitude of the ice content change with the SHAW model and the SHB method for the thawing event is consistent, and ice content changes in the freezing process of the silt loam with $\theta_{L(z,0)} = 0.30$ m^3 m^{-3} showed small maximum absolute differences, at most 0.013 m^3 m^{-3}, for the soil layers below 24 mm. The SHB method estimates of ice content were consistent with the ice estimates of the SHAW model below a depth of 24 mm regardless of soil type and initial soil water content. Soil freezing in many cases penetrates below a depth of 100 mm (e.g., DeGaetano et al., 2001; Flerchinger et al., 2006), which implies that ice content determinations for soil layers below 24 mm are quite important. Therefore, the results indicate that the SHB method can be a powerful tool for investigating long-term soil freezing and thawing events at specific locations.

Effect of Convective Heat Flow on the Sensible Heat Balance Method

The effect of convective heat transfer associated with liquid water flow on ice content estimation in the soil with the SHB method was examined. The heat associated with liquid water flow influencing the SHB method for each soil layer, Q (J m^{-2}), can be determined as

$$\frac{Q}{\Delta t} = \Gamma_{i-1/2}\rho_L c_L q_{L,i-1/2}\left(T_{i-1} - T_i\right) - \Gamma_{i+1/2}\rho_L c_L q_{L,i+1/2}\left(T_{i+1} - T_i\right) \quad [18]$$

where $q_{L,i-1/2}$ and $q_{L,i+1/2}$ are liquid water fluxes (m s^{-1}) at the upper and lower boundaries of the soil layer, positive downward, and Γ is a coefficient to null the term when the liquid water flux is flowing out of the specific layer, i.e., $\Gamma_{i-1/2} = 0$ when $q_{L,i-1/2} < 0$, $\Gamma_{i-1/2} = 1$ when $q_{L,i-1/2} \geq 0$, $\Gamma_{i+1/2} = 0$ when $q_{L,i+1/2} \geq 0$, and $\Gamma_{i+1/2} = 1$ when $q_{L,i+1/2} < 0$. Because changes in the soil volumetric heat capacity, C_s, due to liquid water flow is taken into account in the SHB method, Q is expressed as the product of heat capacity of liquid water, inflowing liquid water flux, and the temperature difference between soil layers. There is no influence of convective heat flux on the SHB method for liquid water flux flowing out of the soil layer. The total Q values of each soil layer after the freezing event and after the thawing event for the sand with $\theta_{L(z,0)} = 0.10$ m^3 m^{-3} and the silt loam with $\theta_{L(z,0)} = 0.30$ m^3 m^{-3} were calculated with Eq. [18] (Table 2). Freezing and thawing periods for each soil layer were defined as the time during which each soil layer experienced temperatures <0°C. The air temperature shifted from freezing to thawing conditions after Day 4 (t = 96 h). The cumulative Q values were always positive because incoming flow generally occurs from warmer soil layers to cooler soil layers under freezing–thawing conditions. In addition, compared with thawing, the freezing process showed larger cumulative Q values, possibly due to larger temperature differences between soil layers during freezing. The equivalent volumetric ice content was calculated by dividing Q by the latent heat of fusion, L_f (334,000 J kg^{-1}), the density of ice (916.7 kg m^{-3}), and the soil layer thickness (0.012 m). The maximum equivalent volumetric ice contents are on the order of 10^{-4} m^3 m^{-3}. The results indicate that conduction was dominant for this freezing and thawing event, and the effect of convective heat transfer associated with liquid water flow on the SHB method for freezing and thawing was negligible, as was found for the SHB method for evaporation and condensation (Sakai et al., 2011).

Table 2. Total heat influencing the sensible heat balance (SHB) method associated with liquid water flow, Q, of each soil layer and its equivalent ice content during freezing and thawing periods with a step change in air temperature conditions.

Soil texture	Initial water content	Layer depth	Q		Equivalent ice content	
			Freezing	Thawing	Freezing	Thawing
	m^3 m^{-3}	mm	J m^{-2}		m^3 m^{-3}	
Sand	0.1	12–24	78	4	2.1×10^{-5}	1.1×10^{-6}
		36–48	71	13	1.9×10^{-5}	3.5×10^{-6}
		60–72	60	10	1.6×10^{-5}	2.6×10^{-6}
		84–96	52	5	1.4×10^{-5}	1.5×10^{-6}
Silt loam	0.3	12–24	1685	69	4.6×10^{-4}	1.9×10^{-5}
		36–48	1452	115	4.0×10^{-4}	3.1×10^{-5}
		60–72	1346	39	3.7×10^{-4}	1.1×10^{-5}
		84–96	1253	24	3.4×10^{-4}	6.4×10^{-6}

Impact of Simultaneous Evaporation–Condensation and Freezing–Thawing on the Sensible Heat Balance Method

The effect of evaporation, sublimation, and condensation during soil freezing and thawing on the SHB method was evaluated. Because evaporation and sublimation are phase changes of water consuming energy, and freezing is a phase change of water releasing energy, concurrent evaporation or sublimation and freezing causes an underestimation of the ice content with the SHB method. In contrast, concurrent condensation and freezing results in an overestimation of ice content with the SHB method because both condensation and freezing are water phase changes that release energy. The latent heat flux at the soil surface (positive upward) associated with surface evaporation, sublimation, and condensation of each soil and initial water content are presented in Fig. 4. The latent heat flux during freezing and thawing was positive except for the moment when the air temperature was switched from −5 to 5°C. This indicates that there was surface evaporation or sublimation during both freezing and thawing. The surface latent heat flux decreased with surface soil freezing and remains at a constant, small value during thawing compared with freezing. The silt loam with an initial water content $\theta_{L(z,0)} = 0.30$ m^3 m^{-3} showed a relatively large latent heat flux during freezing. Cumulative surface latent heat and cumulative latent heat associated with evaporation, sublimation, and condensation for the 0- to 12-, 12- to 24-, 24- to

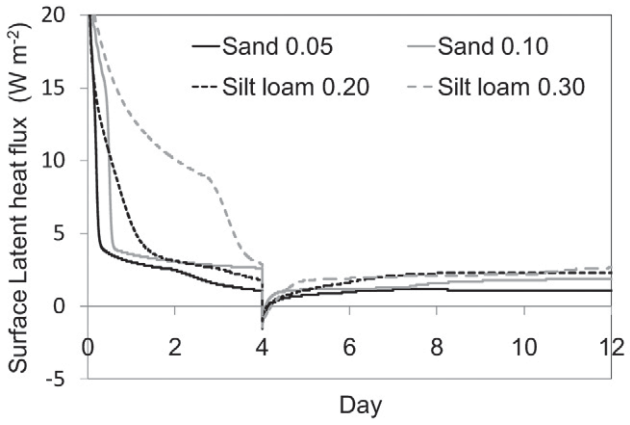

Fig. 4. Surface latent heat fluxes associated with evaporation, sublimation, and condensation (positive upward) for sand with initial water contents of 0.05 and 0.10 $m^3\ m^{-3}$ and silt loam with an initial water content of 0.20 and 0.30 $m^3\ m^{-3}$.

36-, 36- to 48-, 60- to 72-, and 84- to 96-mm soil layers during a freezing and thawing event for the sand with $\theta_{L(z,0)}$ = 0.05 and 0.10 $m^3\ m^{-3}$ and the silt loam with $\theta_{L(z,0)}$ = 0.20 and 0.30 $m^3\ m^{-3}$ are listed in Table 3. Positive latent heat values indicate evaporation or sublimation, and negative values indicate condensation. Freezing and thawing periods of each soil layer correspond to the time that each layer experienced temperatures <0°C. The cumulative surface latent heat and the cumulative latent heat from the 0- to 12-mm soil layer are cumulative values during the time period when the 12- to 24-mm soil layer experienced temperatures <0°C. Equivalent ice contents, which were calculated by dividing the cumulative latent heat associated with vaporization by the latent heat of fusion, the density of ice, and soil layer thickness, are also listed in Table 3. More than 80% of the surface latent heat came from the 0- to 12-mm layer except for the thawing event for the sand with $\theta_{L(z,0)}$ = 0.05 $m^3\ m^{-3}$, and the equivalent ice content of the 0- to 12-mm layer was large relative to deeper layers.

Latent heat due to evaporation and condensation from the 12- to 24-mm layer was small. Although the equivalent ice contents calculated for the 12- to 24-mm layer of the sand with $\theta_{L(z,0)}$ = 0.05 $m^3\ m^{-3}$, 0.0199 and 0.0180 $m^3\ m^{-3}$ for freezing and thawing, respectively, are small, they represent a large fraction of the maximum ice content value, which was 0.031 $m^3\ m^{-3}$. There were small vapor fluxes due to thermal gradients in soil layers deeper than 12 mm; however, the equivalent ice content associated with the latent heat for evaporation and condensation due to vapor transfer in soils is small. Thus, the effect of the latent heat transfer associated with vapor flow on the SHB method was negligible in the soil below a depth of 12 mm.

Table 3. Cumulative latent heat associated with vaporization from the surface and from each soil layer, and the equivalent ice contents during freezing and thawing periods with a step change in air temperature conditions.

Soil texture	Initial water content	Layer depth	Latent heat associated with vaporization		Equivalent ice content	
			Freezing	Thawing	Freezing	Thawing
	$m^3\ m^{-3}$	mm	—— J m^{-2} ——		—— $m^3\ m^{-3}$ ——	
Sand	0.05	at surface	865,218	49,410	–	–
		0–12	719,903	1,668	0.1959	0.0005
		12–24	73,277	65,986	0.0199	0.0180
		24–36	−6,424	−4,297	−0.0017	−0.0012
		36–48	−5,756	−3,980	−0.0016	−0.0011
		60–72	−5,019	−3,449	−0.0014	−0.0009
		84–96	−4,536	−3,076	−0.0012	−0.0008
	0.10	at surface	1,281,720	137,868	–	–
		0–12	1,214,883	157,920	0.3307	0.0430
		12–24	−6,865	−2,601	−0.0019	−0.0007
		24–36	−10,178	−6,613	−0.0028	−0.0018
		36–48	−9,647	−7,305	−0.0026	−0.0020
		60–72	−7,853	−6,880	−0.0021	−0.0019
		84–96	−6,808	−6,833	−0.0019	−0.0019
Silt loam	0.20	at surface	1,520,904	129,024	–	–
		0–12	1,231,754	210,033	0.3353	0.0572
		12–24	789	−11,782	0.0002	−0.0032
		24–36	−5,052	−15,979	−0.0014	−0.0043
		36–48	−3,230	−14,945	−0.0009	−0.0041
		60–72	−676	−13,358	−0.0002	−0.0036
		84–96	1,136	−11,996	0.0003	−0.0033
	0.30	at surface	3,030,618	385,626	–	–
		0–12	2,864,654	443,764	0.7797	0.1208
		12–24	−27,796	−29,382	−0.0076	−0.0080
		24–36	−9,711	−23,182	−0.0026	−0.0063
		36–48	−5,821	−20,943	−0.0016	−0.0057
		60–72	−1,763	−17,946	−0.0005	−0.0049
		84–96	860	−15,034	0.0002	−0.0041

Conductive Heat Fluxes at the Twelve-Millimeter Depth

Table 4 shows cumulative conductive heat flux *H* at the 12-mm depth during the freezing process (Days 0–4) simulated with the SHAW model and calculated with the SHB method. There were large differences between the heat fluxes. The equivalent ice contents associated with these conductive heat differences were calculated by dividing the cumulative conductive heat flux difference by the latent heat of fusion, the ice density, and the soil layer thickness. The equivalent ice contents associated with poorly estimated conductive heat flow by the SHB method were 0.112, 0.123, 0.035, and

Table 4. Cumulative conductive heat (H) at the 12-mm depth during a freezing event (Days 0–4) simulated with the simultaneous heat and water (SHAW) model and estimated with the sensible heat balance (SHB) model.

Soil texture	Initial water content	SHAW H at 12 mm	SHB H at 12 mm	Difference between SHAW H and SHB H	Equivalent ice content
	$m^3\ m^{-3}$	——— J m^{-2} ———			$m^3\ m^{-3}$
Sand	0.05	−8,003,586	−8,413,494	409,908	0.112
	0.10	−11,137,587	−11,589,271	451,684	0.123
Silt loam	0.20	−8,061,513	−8,190,944	129,431	0.035
	0.30	−12,706,251	−14,714,813	2,008,562	0.547

0.547 $m^3\ m^{-3}$ for the sand with $\theta_{L(z,0)}$ = 0.05 and 0.10 $m^3\ m^{-3}$ and the silt loam with $\theta_{L(z,0)}$ = 0.20 and 0.30 $m^3\ m^{-3}$, respectively. These equivalent ice contents were similar to the maximum absolute differences between ice contents simulated with the SHAW model and ice contents calculated with the SHB method for the 12- to 24-mm soil layer, i.e., 0.154, 0.127, 0.035, and 0.444 $m^3\ m^{-3}$ for the sand with $\theta_{L(z,0)}$ = 0.05 and 0.10 $m^3\ m^{-3}$ and the silt loam with $\theta_{L(z,0)}$ = 0.20 and 0.30 $m^3\ m^{-3}$, respectively. Therefore, the reason for the inaccurate determinations of ice contents in the 12- to 24-mm soil layer was mainly caused by poor estimates of the conductive heat flux at the 12-mm depth by the SHB method. Assumptions and numerical instabilities inherent in simulating the nonlinear changes in mass, temperature, and thermal properties near the surface during freezing can introduce errors in the SHAW model simulation. Therefore, the SHB method's poor estimate of 12-mm-depth conductive heat flow in comparison to the SHAW model may not entirely be due to limitations of the SHB method. When the SHAW model conductive heat flux at 12 mm is considered as a standard, however, a possible reason for the inaccurate estimation of conductive heat flux may be the continuous changes in T and λ_s within the 15-min time intervals being simplified as a step change in the SHB method along with the simplification of the vertical distribution of temperature and thermal conductivities by the SHB method. Finer spatial and temporal intervals for the SHB method may be required to improve estimates in soil layers shallower than 24 mm.

Sensible Heat Balance Application under Transient Atmospheric Conditions

The transient atmospheric conditions (T_a, RH_a, u, R_s, and P) used to determine the surface boundary conditions for water and heat transfer are shown in Fig. 5. A daily soil freezing and thawing cycle occurred in response to the transient weather conditions. The ice content transition estimated with SHB method and calculated with the SHAW model and the temperatures for the 12- to 24-, 36- to 48-, 60- to 72-, and 84- to 96-mm soil layers are shown in Fig. 6. Daily freezing events occurred at around 0400 h and were maintained until around 1200 h. While freezing penetration was

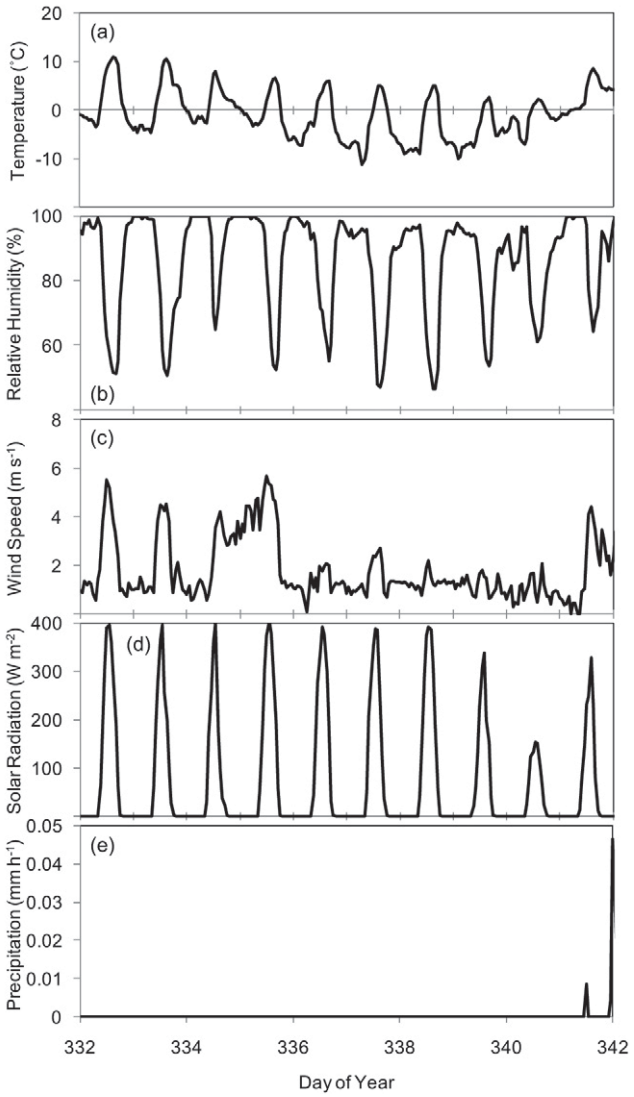

Fig. 5. Transient atmospheric conditions: (a) air temperature, (b) relative humidity, (c) wind speed, (d) solar radiation, and (e) precipitation rate. The data were taken from Flerchinger et al. (2006).

not significant at the beginning of the period, it extended below the 10-cm depth after DOY 337 to 341. The maximum ice contents were about 0.06 $m^3\ m^{-3}$ throughout the period. The maximum absolute differences between the SHAW model and the SHB method were 0.018, 0.010, 0.007, and 0.008 $m^3\ m^{-3}$ for the 12- to 24-, 36- to 48-, 60- to 72-, and 84- to 96-mm soil layers. The SHB estimation captured the daily ice content transitions with depth and time. Moreover, clear agreements between ice content transitions calculated with the SHAW model and those determined by the SHB method were obtained for each soil layer including the 12- to 24-mm layer. The SHB balance method is conceptually suitable for diurnal freezing and thawing events under natural atmospheric conditions.

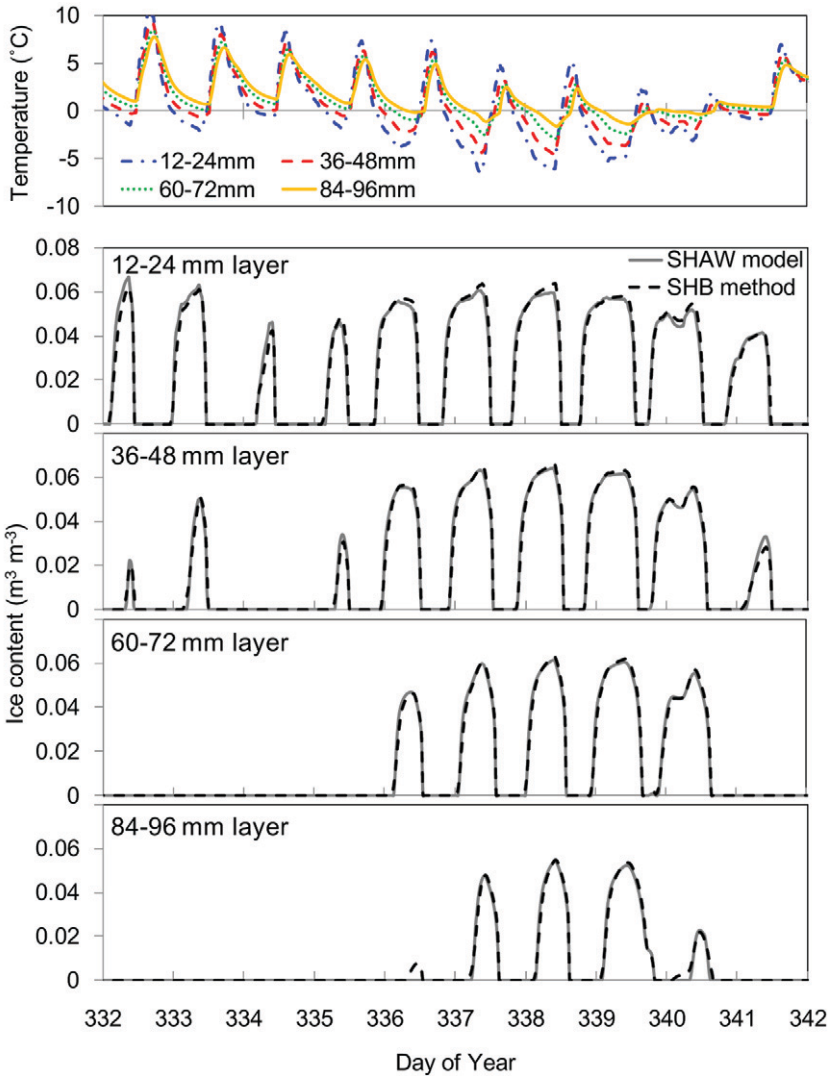

Fig. 6. Temperature at the mid-depth of the 12- to 24-, 36- to 48-, 60- to 72-, and 84- to96-mm soil layers simulated with the simultaneous heat and water (SHAW) model (upper) and volumetric ice contents simulated with the SHAW model (solid lines) and calculated with the sensible heat balance (SHB) method (dashed lines) for the 12- to 24-, 36- to 48-, 60- to 72-, and 84- to96-mm soil layers (lower) for the transient atmospheric condition study.

Conclusions

The SHB method has been previously applied for measuring condensation and evaporation in unfrozen soil. The applicability and potential limitations of the SHB method for measuring soil ice content changes were investigated by applying the SHB concept to data numerically produced with the SHAW model. The results of this numerical study indicate that the SHB method is conceptually suitable for estimating ice formation and thawing in subsurface soil layers for long-term freezing and thawing events with the assumption that the heat pulse probes can accurately determine the thermal conductivity and heat capacity in frozen soils. The only limitation on the SHB was for use on the 0- to 24-mm surface soil layer due to poor estimation of conductive heat fluxes at the 12-mm depth during soil freezing. These poor estimations may have been due to the continuous changes and vertical distributions of thermal conductivities and temperatures, which are simplified in the SHB. From simulations of diurnally varying conditions, the SHB method was also demonstrated as being suitable for estimating daily freezing and thawing events. Convective heat transfer associated with liquid water flow had negligible impacts on the SHB estimations. The effects of simultaneous evaporation or sublimation and condensation occurring with freezing on the SHB estimates of ice contents were small in the soil layers deeper than 12 mm. The SHB method should be further tested by making actual measurements in freezing and thawing soils.

Acknowledgments

This work was supported by the National Science Foundation under Grants 0809656 and 1215864 and by the Hatch Act, State of Iowa, and State of North Carolina funds. We acknowledge Dr. Robert Ewing, Iowa State University, for helpful discussions.

References

Bittelli, M., M. Flury, and G.S. Campbell. 2003. A thermodielectric analyzer to measure the freezing and moisture characteristic of porous media. Water Resour. Res. 39(2):1041. doi:10.1029/2001WR000930

Bittelli, M., M. Flury, and K. Roth. 2004. Use of dielectric spectroscopy to estimate ice content in frozen porous media. Water Resour. Res. 40:W04212. doi:10.1029/2003WR002343

Bristow, K.L., G.J. Kluitenberg, and R. Horton. 1994. Measurement of soil thermal properties with a dual-probe heat-pulse technique. Soil Sci. Soc. Am. J. 58:1288–1294. doi:10.2136/sssaj1994.03615995005800050002x

Campbell, G.S. 1974. A simple method for determining unsaturated conductivity from moisture retention data. Soil Sci. 117:311–314. doi:10.1097/00010694-197406000-00001

Campbell, G.S., C. Calissendorff, and J.H. Williams. 1991. Probe for measuring soil specific heat using a heat-pulse method. Soil Sci. Soc. Am. J. 55:291–293. doi:10.2136/sssaj1991.03615995005500010052x

Campbell, G.S., and J.M. Norman. 1998. An introduction to environmental biophysics. 2nd ed. Springer, New York.

Cary, J.W., and H.F. Mayland. 1972. Salt and water movement in unsaturated frozen soil. Soil Sci. Soc. Am. J. 36:549–555. doi:10.2136/sssaj1972.03615995003600040019x

Cary, J.W., R.I. Papendick, and G.S. Campbell. 1979. Water and salt movement in unsaturated frozen soil: Principles and field observation. Soil Sci. Soc. Am. J. 43:3–8. doi:10.2136/sssaj1979.03615995004300010001x

Cruse, R.M., R. Mier, and C.W. Mize. 2001. Surface residue effects on erosion of thawing soils. Soil Sci. Soc. Am. J. 65:178–184. doi:10.2136/sssaj2001.651178x

DeGaetano, A.T., M.D. Cameron, and D.S. Wilks. 2001. Physical simulation of maximum seasonal soil freezing depth in the United States using routine weather observations. J. Appl. Meteorol. 40:546–555. doi:10.1175/1520-0450(2001)040<0546:PSOMSS>2.0.CO;2

de Vries, D.A. 1963. Thermal properties of soils. In: W.R. van Wijk, editor, Physics of plant environment. 2nd ed. North Holland Publ., Amsterdam. p. 210–235.

Dirksen, C., and R.D. Miller. 1966. Closed-system freezing of unsaturated soil. Soil Sci. Soc. Am. J. 30:168–173. doi:10.2136/sssaj1966.03615995003000020010x

Flerchinger, G.N., and S.P. Hardegree. 2004. Modeling near-surface soil temperature and moisture for germination response predictions of post-wildfire seedbeds. J. Arid Environ. 59:369–385. doi:10.1016/j.jaridenv.2004.01.016

Flerchinger, G.N., and K.E. Saxton. 1989a. Simultaneous heat and water model of a freezing snow–residue–soil system: I. Theory and development. Trans. ASAE 32:565–571.

Flerchinger, G.N., and K.E. Saxton. 1989b. Simultaneous heat and water model of a freezing snow–residue–soil system: II. Field verification. Trans. ASAE 32:573–578.

Flerchinger, G.N., M.S. Seyfried, and S.P. Hardegree. 2006. Using soil freezing characteristics to model multi-season soil water dynamics. Vadose Zone J. 5:1143–1153. doi:10.2136/vzj2006.0025

Fuchs, M., G.S. Campbell, and R.I. Papendick. 1978. An analysis of sensible and latent heat flow in a partially frozen unsaturated soil. Soil Sci. Soc. Am. J. 42:379–385. doi:10.2136/sssaj1978.03615995004200030001x

Fukuda, M. 1983. Experimental studies of coupled heat and moisture transfer in soils during freezing. Contrib. Inst. Low Temp. Sci., Hokkaido Univ. A31:35–91.

Fukuda, M., and S. Kinosita. 1985. Field frost heave prediction related to ice segregation processes during soil freezing. Ann. Glaciol. 6:87–91.

Galinato, G.J. 1987. Soil moisture and nitrate movement under freezing conditions. Ph.D. diss. Iowa State Univ., Ames.

Gieselman, H., J.L. Heitman, and R. Horton. 2008. Effect of a hydrophobic layer on the upward movement of water under surface freezing conditions. Soil Sci. 173:297–305. doi:10.1097/SS.0b013e31816d1e75

Hayhoe, H.N., and W.G. Bailey. 1985. Monitoring changes in total and unfrozen water content in seasonally frozen soil using time domain reflectometry and neutron moderation techniques. Water Resour. Res. 21:1077–1084. doi:10.1029/WR021i008p01077

Hayhoe, H.N., G.C. Topp, and W.G. Bailey. 1983. Measurement of soil water contents and frozen soil depth during a thaw using time-domain reflectometry. Atmos.-Ocean 21:299–311. doi:10.1080/07055900.1983.9649170

Heitman, J.L., R. Horton, T. Ren, I.N. Nassar, and D.D. Davis. 2008b. A test of coupled soil heat and water transfer prediction under transient boundary temperatures. Soil Sci. Soc. Am. J. 72:1197–1207. doi:10.2136/sssaj2007.0234

Heitman, J.L., R. Horton, T.J. Sauer, and T.M. DeSutter. 2008a. Sensible heat observations reveal soil water evaporation dynamics. J. Hydrometeorol. 9:165–171. doi:10.1175/2007JHM963.1

Heitman, J.L., X. Xiao, R. Horton, and T.J. Sauer. 2008c. Sensible heat measurements indicating depth and magnitude of subsurface soil water evaporation. Water Resour. Res. 44:W00D05. doi:10.1029/2008WR006961

Kahimba, F.C., and R. Sri Ranjan. 2007. Soil temperature correction of field TDR readings obtained under near freezing conditions. Can. Biosyst. Eng. 49:1.19–1.26.

Kane, D.L., and J. Stein. 1983. Water movement into seasonally frozen soils. Water Resour. Res. 19:1547–1557. doi:10.1029/WR019i006p01547

Kelleners, T.J., and J.B. Norton. 2012. Determining water retention in seasonally frozen soils using Hydra impedance sensors. Soil Sci. Soc. Am. J. 76:36–50. doi:10.2136/sssaj2011.0222

Kluitenberg, G.J., K.L. Bristow, and B.S. Das. 1995. Error analysis of heat pulse method for measuring soil heat capacity, diffusivity, and conductivity. Soil Sci. Soc. Am. J. 59:719–726. doi:10.2136/sssaj1995.03615995005900030013x

Koopmans, R.W.R., and R.D. Miller. 1966. Soil freezing and soil water characteristic curves. Soil Sci. Soc. Am. J. 30:680–685. doi:10.2136/sssaj1966.03615995003000060011x

Kung, S.K.J., and T.S. Steenhuis. 1986. Heat and moisture transfer in a partly frozen nonheaving soil. Soil Sci. Soc. Am. J. 30:1114–1122. doi:10.2136/sssaj1986.03615995005000050005x

Liu, G., and B.C. Si. 2011. Soil ice content measurement using a heat pulse probe method. Can. J. Soil Sci. 91:235–246. doi:10.4141/cjss09120

Loch, J.P.G., and B.D. Kay. 1978. Water redistribution in partially frozen, saturated silt under several temperature gradients and overburden loads. Soil Sci. Soc. Am. J. 42:400–406. doi:10.2136/sssaj1978.03615995004200030005x

Miller, R.D. 1972. Freezing and heaving of saturated and unsaturated soils. Highw. Res. Rec. 393:1–11.

Nassar, I.N., R. Horton, and G.N. Flerchinger. 2000. Simultaneous heat and mass transfer in soil columns exposed to freeing/thawing conditions. Soil Sci. 165:208–216. doi:10.1097/00010694-200003000-00003

Ochsner, T.E., and J.M. Baker. 2008. In situ monitoring of soil thermal properties and heat flux during freezing and thawing. Soil Sci. Soc. Am. J. 72:1025–1032. doi:10.2136/sssaj2007.0283

Ochsner, T.E., R. Horton, and T. Ren. 2001. A new perspective on soil thermal properties. Soil Sci. Soc. Am. J. 65:1641–1647. doi:10.2136/sssaj2001.1641

Overduin, P.P., D.L. Kane, and W.K.P. van Loon. 2006. Measuring thermal conductivity in freezing and thawing soil using the soil temperature response to heating. Cold Reg. Sci. Technol. 45:8–22. doi:10.1016/j.coldregions.2005.12.003

Penner, E. 1967. Heaving pressure in soils during unidirectional freezing. Can. Geotech. J. 4:398–408. doi:10.1139/t67-067

Penner, E. 1970. Thermal conductivity of frozen soils. Can. J. Earth Sci. 7:982–987. doi:10.1139/e70-091

Putkonen, J. 2003. Determination of frozen soil thermal properties by heated needle probe. Permafrost Periglac. Processes 14:343–347. doi:10.1002/ppp.465

Sakai, M., S.B. Jones, and M. Tuller. 2011. Numerical evaluation of subsurface soil water evaporation derived from sensible heat balance. Water Resour. Res. 47:W02547. doi:10.1029/2010WR009866

Sartz, R.S. 1969. Soil water movement as affected by deep freezing. Soil Sci. Soc. Am. J. 33:333–337. doi:10.2136/sssaj1969.03615995003300030005x

Seyfried, M.S., and M.D. Murdock. 1996. Calibration of time domain reflectometry for measurement of liquid water in frozen soils. Soil Sci. 161:87–98. doi:10.1097/00010694-199602000-00002

Spaans, E.J.A., and J.M. Baker. 1995. Examining the use of time domain reflectometry for measuring liquid water content in frozen soil. Water Resour. Res. 31:2917–2925. doi:10.1029/95WR02769

Stein, J., and D.L. Kane. 1983. Monitoring the unfrozen water content of soil and snow using time domain reflectometry. Water Resour. Res. 19:1573–1584. doi:10.1029/WR019i006p01573

Tokumoto, I., K. Noborio, and K. Koga. 2010. Coupled water and heat flow in a grass field with aggregated Andisol during soil-freezing periods. Cold Reg. Sci. Technol. 62:98–106. doi:10.1016/j.coldregions.2010.03.005

Wagner-Riddle, C., J. Rapai, J. Warland, and A. Furon. 2010. Nitrous oxide fluxes related to soil freeze and thaw periods identified using heat pulse probes. Can. J. Soil Sci. 90:409–418. doi:10.4141/CJSS09016

Watanabe, K., Y. Oomori, T. Wake, and M. Sakai. 2010. Simultaneous measurements of water content and thermal conductivity of frozen soils by using thermo-TDR method. (In Japanese.) Seppyo 72:157–168.

Watanabe, K., and K. Wake. 2009. Measurement of unfrozen water content and relative permittivity of frozen unsaturated soil using NMR and TDR. Cold Reg. Sci. Technol. 59:34–41. doi:10.1016/j.coldregions.2009.05.011

Williams, P.J. 1964. Unfrozen water content of frozen soils and soil moisture suction. Geotechnique 14:231–246. doi:10.1680/geot.1964.14.3.231

Xiao, X., R. Horton, T.J. Sauer, J.L. Heitman, and T. Ren. 2011. Cumulative soil water evaporation as a function of depth and time. Vadose Zone J. 10:1016–1022. doi:10.2136/vzj2010.0070

Zhang, Y., M. Treberg, and S.K. Carey. 2011. Evaluation of the heat probe method for determining frozen soil moisture content. Water Resour. Res. 47:W05544. doi:10.1029/2010WR010085